

Sensing Matrix Design and Sparse Recovery on the Sphere and the Rotation Group

Arya Bangun, Arash Behboodi, and Rudolf Mathar*

Abstract

In this paper, the goal is to design random or regular samples on the sphere or the rotation group and, thereby, construct sensing matrices for sparse recovery of band-limited functions. It is first shown that random sensing matrices, which consists of random samples of Wigner D-functions, satisfy the Restricted Isometry Property (RIP) with a proper preconditioning and can be used for sparse recovery on the rotation group. The mutual coherence, however, is used to assess the performance of deterministic and regular sensing matrices. We show that many of widely used regular sampling patterns yield sensing matrices with the worst possible mutual coherence, and therefore are undesirable for sparse recovery. Using tools from angular momentum analysis in quantum mechanics, we provide a new expression for the mutual coherence, which encourages the use of regular elevation samples. We construct low coherence deterministic matrices by fixing the regular samples on the elevation and minimizing the mutual coherence over the azimuth-polarization choice. It is shown that once the elevation sampling is fixed, the mutual coherence has a lower bound that depends only on the elevation samples. This lower bound, however, can be achieved for spherical harmonics, which leads to new sensing matrices with better coherence than other representative regular sampling patterns. This is reflected as well in our numerical experiments where our proposed sampling patterns match perfectly the phase transition of random sampling patterns.

1 Introduction

In many applications, where the goal is to recover a sparse signal from the fewest linear measurements, the measurement process cannot be freely chosen. That is, in the corresponding linear inverse problem, the sensing matrix has a specific structure. A central question, therefore, is to design the sensing matrix under these additional restrictions.

For general sensing matrices, the pioneering works of compressed sensing [1–3] followed by overwhelming subsequent researches established recovery guarantees for various random matrices including subgaussian random matrices. These random matrices are shown to satisfy, with high probability, the Restricted Isometry Property (RIP), which is a sufficient condition for noise-robust sparse recovery. Many efficient algorithms such as Basis Pursuit (BP) can provably recover the original signal from these measurements (see [4] for an exhaustive treatment of the subject).

In contrast to pure random matrix designs, in many applications, the sensing medium imposes additional structures on sensing matrices. Notable examples are sensing matrices that are obtained from sampling functions in finite-dimensional function spaces. The sensing matrix entries in these applications are samples of orthonormal basis functions of the ambient space. Fourier matrices [5], matrices from trigonometric polynomials [6], orthogonal polynomials [7, 8] and spherical harmonics [9, 10] are some examples of these matrices. Fortunately, when the orthonormal functions are uniformly bounded, also called Bounded Orthonormal Systems (BOSs), a similar recovery guarantee can be obtained. If the samples are taken randomly from a certain probability measure, BOS matrices are proven to satisfy the RIP property [4, Chapter 12]. If the orthonormal functions are uniformly bounded by K , the required number of measurements scales with K^2 .

This randomness in the measurement process, however, is inadmissible in many applications, for instance when the measurement process involves movements of mechanical devices. Random measurements require arbitrary movements that are possibly harmful to the measurement device. In these applications, the measurement process should be designed by considering the physical characteristics of the measurement device. An example, which is the main motivation of the current work, is the antenna measurement application. The samples in antenna measurements are taken using a robotic arm or which

*Institute for Theoretical Information Technology, RWTH Aachen University

samples of a smooth trajectory are preferred over random samples. Therefore, regular sampling patterns like equiangular patterns are widely used for the measurement process. The desired sensing matrices should be both structured, since it involves samples of orthonormal functions, and deterministic, which should bring about regular sampling patterns. In this paper, our goal is to address these requirements step by step for sparse recovery in the space of band-limited square-integrable functions over the sphere \mathbb{S}^2 and the rotation group $\text{SO}(3)$. These functions appear in wide range of applications such as antenna measurements [11], geophysics [12], spherical microphone arrays [13], and astrophysics [14].

Consider random measurements first. The orthonormal functions over \mathbb{S}^2 and $\text{SO}(3)$ are spherical harmonics and Wigner D-functions, random samples of which constitutes the entries of the sensing matrix. The upper bound of these functions, K , is a function of the ambient dimension N . When it is plugged in the recovery guarantees for BOSs, it would imply that the number of measurements should scale badly with the dimension N . This bound is useless for sparse recovery analysis. Rauhut and Ward used a preconditioning technique in [9] and improved the dependence to $N^{1/4}$. Burq et al. improved this further to $N^{1/6}$ in [10]. These results, however, do not directly generalize to Wigner D-functions.

As soon as we move to deterministic sampling patterns, the RIP cannot be used to appraise the sparse recovery capability of the sensing matrices. It is computationally hard to certify that a certain matrix satisfies RIP [15, 16]. A common metric for deterministic sensing matrices is the mutual coherence. It is defined as the maximum of the absolute value of normalized inner products between columns of the sensing matrix. Unlike RIP, the mutual coherence can be numerically evaluated for a given matrix, and therefore it is a computable figure of merit for sparse recovery. The mutual coherence of a matrix can be also used to provide recovery guarantees, although it leads to a suboptimal dependence on the sparsity order. In general, sensing matrices with low mutual coherence tend to have better sparse recovery performance. Therefore, constructing a sensing matrix with low mutual coherence has been widely investigated in recent years because of its extensive application in many different areas, from coding theory [17–19], communication [17, 20], compressed sensing [2, 3, 21–23], phase retrieval [24], quantum measurement [25], [26] and machine learning [27, 28]. The mutual coherence is lower bounded by the Welch bound, obtained in the context of correlation measurements of different signals [29]. The lower bound is tight and can be achieved by equiangular and tight frames [17]. A similar result for structured matrices is not known to the best of our knowledge. Deterministic sampling patterns on the sphere \mathbb{S}^2 have been studied extensively in context of Shannon-Nyquist sampling for reconstruction of band-limited functions (see [30–32] and references therein). As mentioned by McEwen and Wiaux in [30], some of these techniques can be used to enhance the performance of compressed sensing methods. Equiangular sampling patterns are often the standard in these applications. We will see, however, that equiangular sampling patterns are not the best choice from compressed sensing perspective.

Compressed sensing on the sphere was considered in [33]. Alem et al. proposed random samples from a spiral on the sphere that outperforms the equiangular sampling. A modification of equiangular sampling patterns was proposed as well in [34]. They further extended the result of [10] for probabilistic compressed sensing and derived similar bounds in [35]. These results are all based on random sampling.

1.1 Summary of Contributions

In this paper, we consider the problem of sensing matrix design and evaluation for sparse recovery of band-limited functions on the sphere \mathbb{S}^2 and the rotation group $\text{SO}(3)$. The sensing matrix design boils down to finding m sampling points $(\theta, \phi) \in \mathbb{S}^2$ and $(\theta, \phi, \chi) \in \text{SO}(3)$, where $\theta \in [0, \pi]$, $\phi \in [0, 2\pi)$ and $\chi \in [0, 2\pi)$. The main contributions of our paper are as follows.

- In Section 3, we prove that sparse band-limited signals over the rotation group $\text{SO}(3)$ can be uniquely recovered from certain random sampling patterns by solving a convex optimization problem. The proof follows from the RIP property of the sensing matrix after preconditioning, which is based on some inequalities for Jacobi polynomials. The recovery algorithm is robust to noise and stable to model inaccuracies.
- Adopting the mutual coherence as the figure of merit from Section 4, we show that certain regular deterministic sampling patterns over the sphere and the rotation group with symmetric structures over ϕ and χ have maximum coherence and, therefore, are not good for sparse recovery. These patterns include many of sampling patterns that are currently widely used in applications including equiangular sampling patterns.
- The mutual coherence is determined by the inner products of vectors of samples of spherical harmonics and Wigner D-functions. We show in Section 4 that the product of two functions

can be seen as the total angular momentum of a composite quantum system. Borrowing this insight from quantum mechanics, the product can be decomposed into a sum of single spherical harmonics and Wigner D-functions using Wigner 3j symbols. To the best of our knowledge, this decomposition is used for the first time for coherence analysis in compressed sensing. We use the above decomposition to derive regular sampling patterns that lead to mutually orthogonal, and therefore incoherent, columns in the sensing matrix.

- In Section 5, we propose equispaced sampling patterns on θ , which also leads to incoherence columns. We show that once the sampling points on θ is fixed the mutual coherence is automatically lower bounded independent of the choice of ϕ 's and χ 's. It is, however, shown that the lower bound can be achieved for spherical harmonics by using pattern search algorithm. The algorithm minimizes the mutual coherence by choosing appropriately ϕ 's. Although the lower bound cannot be achieved for Wigner D-functions using this method, the mutual coherence of our proposed pattern is still superior to the representative regular sampling patterns. Our phase transition diagrams in Section 6 suggest that our proposed pattern not only outperforms the representative regular patterns, but matches perfectly random sampling patterns.

The codes and sampling points used in this paper are available below:

github.com/bangunarya/samplingsphere

1.2 Notation

The vectors are denoted by bold small-cap letters. Define $\mathbb{N} := \{1, 2, \dots\}$ and $\mathbb{N}_0 := \mathbb{N} \cup \{0\}$. Throughout the paper, $a \lesssim b$ means that there is a universal constant C such that $a \leq Cb$. Similar convention is used for $a \gtrsim b$. $f(\mathbf{x})$ for a function $f: \mathbb{R} \rightarrow \mathbb{R}$ is the element-wise application of f to the vector \mathbf{x} . \bar{x} is the conjugate of x .

2 Definitions and Backgrounds

In this section, we introduce briefly the preliminaries of signal processing over the sphere and the rotation group as well as the problem formulation. The central problem of this work is the recovery of band-limited functions defined on the sphere and the rotation group. We need, therefore, to introduce Fourier analysis for these spaces of functions.

2.1 Spherical Harmonics and Wigner D-functions

Consider the Hilbert space of square-integrable functions $f(\cdot)$ on the sphere \mathbb{S}^2 denoted by $L^2(\mathbb{S}^2)$. Each element of \mathbb{S}^2 is represented by two numbers $\theta \in [0, \pi]$ and $\phi \in [0, 2\pi)$. The variables θ and ϕ are called the elevation and the azimuth. The inner product of $f, g \in L^2(\mathbb{S}^2)$ is defined by

$$\langle f, g \rangle := \int_{\mathbb{S}^2} f(\theta, \phi) \overline{g(\theta, \phi)} d\nu(\theta, \phi),$$

where $d\nu(\theta, \phi) := \sin \theta d\theta d\phi$ is the uniform measure on the sphere. Spherical harmonics are basis functions for the space of functions in $L^2(\mathbb{S}^2)$. Denoted by $Y_l^k(\theta, \phi)$ for degree $l \in \mathbb{N}_0$ and order $k \in \{-l, \dots, l\}$, they are defined over the sphere \mathbb{S}^2 as follows:

$$Y_l^k(\theta, \phi) := N_l^k P_l^k(\cos \theta) e^{ik\phi}, \quad (1)$$

where $P_l^k(\cos \theta)$ is the associated Legendre polynomials defined by

$$P_l^k(x) := \frac{(-1)^k}{2^l l!} (1 - x^2)^{k/2} \frac{d^{k+l}}{dx^{k+l}} (x^2 - 1)^l.$$

The term $N_l^k := \sqrt{\frac{2l+1}{4\pi} \frac{(l-k)!}{(l+k)!}}$ is a normalization factor. It ensures that the function Y_l^k has unit L_2 -norm. Spherical harmonics are orthonormal with respect to the uniform measure on the sphere $d\nu = \sin \theta d\theta d\phi$, i.e.,

$$\int_0^{2\pi} \int_0^\pi Y_l^k(\theta, \phi) \overline{Y_{l'}^{k'}(\theta, \phi)} \sin \theta d\theta d\phi = \delta_{ll'} \delta_{kk'} \quad (2)$$

where $\delta_{ll'}$ is the Kronecker delta. The function $\overline{Y_l^k}$ is the conjugate of Y_l^k and satisfies:

$$\overline{Y_l^k(\theta, \phi)} = (-1)^k Y_l^{-k}(\theta, \phi).$$

For any function $f \in L^2(\mathbb{S}^2)$, the unique expansion

$$f(\theta, \phi) = \sum_{l=0}^{\infty} \sum_{k=-l}^l \hat{f}_l^k Y_l^k(\theta, \phi), \quad (3)$$

where

$$\hat{f}_l^k = \int_0^{2\pi} \int_0^\pi f(\theta, \phi) \overline{Y_l^k(\theta, \phi)} \sin \theta d\theta d\phi. \quad (4)$$

is called the \mathbb{S}^2 -Fourier expansion of f with Fourier coefficients \hat{f}_l^k .

The space of all rotations of the sphere \mathbb{S}^2 is a group called the rotation group and is denoted by $\text{SO}(3)$. Each element of $\text{SO}(3)$ can be represented by three rotation angles $\phi \in [0, 2\pi)$, $\theta \in [0, \pi]$, and $\chi \in [0, 2\pi)$. In this work, we call the angle χ the polarization. The Hilbert space of square integrable functions on $\text{SO}(3)$, denoted by $L^2(\text{SO}(3))$, is endowed with an inner product, which is defined for two functions $f, g \in \text{SO}(3)$ by

$$\langle f, g \rangle := \int_{\text{SO}(3)} f(\theta, \phi, \chi) \overline{g(\theta, \phi, \chi)} d\nu(\theta, \phi, \chi),$$

where $d\nu(\theta, \phi, \chi) := \sin \theta d\theta d\phi d\chi$. Wigner D-functions are an orthonormal basis for the Hilbert space $L^2(\text{SO}(3))$. Denoted by $D_l^{k,n}(\theta, \phi, \chi)$ with degree $l \in \mathbb{N}_0$ and orders $k, n \in \{-l, \dots, l\}$, they are defined by

$$D_l^{k,n}(\theta, \phi, \chi) = N_l e^{-ik\phi} d_l^{k,n}(\cos \theta) e^{-in\chi} \quad (5)$$

where $N_l = \sqrt{\frac{2l+1}{8\pi^2}}$ is the normalization factor to guarantee that Wigner D-functions are unit norm. The function $d_l^{k,n}(\cos \theta)$ is the Wigner d-function of order l and degrees k, n defined by:

$$d_l^{k,n}(\cos \theta) = \omega \sqrt{\gamma} \sin^\xi \left(\frac{\theta}{2} \right) \cos^\lambda \left(\frac{\theta}{2} \right) P_\alpha^{(\xi, \lambda)}(\cos \theta) \quad (6)$$

where $\gamma = \frac{\alpha!(\alpha+\xi+\lambda)!}{(\alpha+\xi)!(\alpha+\lambda)!}$, $\xi = |k-n|$, $\lambda = |k+n|$, $\alpha = l - \left(\frac{\xi+\lambda}{2}\right)$ and

$$\omega = \begin{cases} 1 & \text{if } n \geq k \\ (-1)^{n-k} & \text{if } n < k \end{cases}.$$

The function $P_\alpha^{(\xi, \lambda)}$ is the Jacobi polynomial. The orthonormal property of Wigner D-functions writes as:

$$\begin{aligned} \int_0^{2\pi} \int_0^{2\pi} \int_0^\pi D_l^{k,n}(\theta, \phi, \chi) \overline{D_{l'}^{k',n'}(\theta, \phi, \chi)} \sin \theta d\theta d\phi d\chi \\ = \delta_{ll'} \delta_{kk'} \delta_{nn'}. \end{aligned} \quad (7)$$

The conjugate of $D_l^{k,n}$ satisfies [36, eq. 7.134]

$$\overline{D_l^{k,n}(\theta, \phi, \chi)} = (-1)^{k-n} D_l^{-k,-n}(\theta, \phi, \chi).$$

The $\text{SO}(3)$ -Fourier expansion of the function $g \in L^2(\text{SO}(3))$ is defined by

$$g(\theta, \phi, \chi) = \sum_{l=0}^{\infty} \sum_{k=-l}^l \sum_{n=-l}^l \hat{g}_l^{k,n} D_l^{k,n}(\theta, \phi, \chi), \quad (8)$$

with Fourier coefficients $\hat{g}_l^{k,n}$ are obtained by

$$\hat{g}_l^{k,n} = \int_0^{2\pi} \int_0^{2\pi} \int_0^\pi g(\theta, \phi, \chi) \overline{D_l^{k,n}(\theta, \phi, \chi)} \sin \theta d\theta d\phi d\chi. \quad (9)$$

An interested reader can refer to the book [37] for more information on Wigner D-functions and $\text{SO}(3)$.

Remark 1. If the order n is set to zero, we get spherical harmonics. The Wigner D-functions $D_l^{k,0}$ for $n = 0$ are related to spherical harmonics Y_l^k as

$$D_l^{-k,0}(\theta, \phi, 0) = (-1)^k \sqrt{\frac{1}{2\pi}} Y_l^k(\theta, \phi). \quad (10)$$

2.2 Sparse Expansions of Band-limited Functions

In this work, we are interested in band-limited functions inside $L^2(\mathbb{S}^2)$. A function $f \in L^2(\mathbb{S}^2)$ is band-limited with bandwidth B if it is expressed in terms of spherical harmonics of degree less than B :

$$f(\theta, \phi) = \sum_{l=0}^{B-1} \sum_{k=-l}^l \hat{f}_l^k Y_l^k(\theta, \phi).$$

The space of band-limited functions with the degree less than B is a subspace of $L^2(\mathbb{S}^2)$ of dimension $N = B^2$. Every band-limited function f , therefore, is fully determined by the vector of N Fourier coefficients $\mathbf{f} = (\hat{f}_l^k)_{0 \leq l < B}$.

We can define similarly the notion of band-limited functions on $\text{SO}(3)$. A function $g \in L^2(\text{SO}(3))$ is band-limited with bandwidth B if it is expressed in terms of Wigner D-functions of degree less than B :

$$g(\theta, \phi, \chi) = \sum_{l=0}^{B-1} \sum_{k=-l}^l \sum_{n=-l}^l \hat{g}_l^{k,n} D_l^{k,n}(\theta, \phi, \chi).$$

The space of band-limited functions with the degree less than B is a subspace of $L^2(\text{SO}(3))$ of dimension $N = \frac{B(2B-1)(2B+1)}{3}$ where each function is completely determined by the vector of Fourier coefficients, $\mathbf{g} = (\hat{g}_l^{k,n})_{0 \leq l < B}$.

A band-limited function, whether in $L^2(\mathbb{S}^2)$ or in $L^2(\text{SO}(3))$, is said to be s -sparse if its coefficient vector \mathbf{x} has at most s non-zero entries. This is stated in terms of the ℓ_0 -norm¹ as $\|\mathbf{x}\|_0 \leq s$. For the general non-sparse vector of coefficients \mathbf{x} , either in $L^2(\mathbb{S}^2)$ or in $L^2(\text{SO}(3))$, the best s -sparse approximation error of \mathbf{x} is defined by:

$$\sigma_s(\mathbf{x})_p = \min_{\mathbf{z} \in \mathbb{C}^N: \|\mathbf{z}\|_0 \leq s} \|\mathbf{z} - \mathbf{x}\|_p.$$

In many applications, the signals are approximately sparse or compressible, that is, the s -sparse approximation error decreases rapidly as s increases.

2.3 Linear Inverse Problems and the ℓ_1 -minimization

Consider a band-limited function either in \mathbb{S}^2 or $\text{SO}(3)$. The function belongs to a finite-dimensional vector space and can be represented by its Fourier coefficients. It is therefore enough to find the Fourier coefficients, a finite-dimensional vector, to specify the function.

We want to find the Fourier coefficients of a band-limited function from noisy linear samples of the function using as few samples as possible. We focus on $\text{SO}(3)$, which contains \mathbb{S}^2 as a special case. Consider a function $g \in L^2(\text{SO}(3))$. We obtain m noisy samples y_p of the function g at points $(\theta_p, \phi_p, \chi_p)$ for $p \in [m]$. The samples are given by:

$$\begin{aligned} y_p &= g(\theta_p, \phi_p, \chi_p) + \eta_p \\ &= \sum_{l=0}^{B-1} \sum_{k=-l}^l \sum_{n=-l}^l \hat{g}_l^{k,n} D_l^{k,n}(\theta_p, \phi_p, \chi_p) + \eta_p, \end{aligned}$$

where η_p is the additive noise with $|\eta_p| \leq \epsilon$. The noisy samples are therefore linearly related to the coefficients $\mathbf{g} = (\hat{g}_l^{k,n})_{0 \leq l < B}$ as follows:

$$\mathbf{y} = \mathbf{A}\mathbf{g} + \boldsymbol{\eta}, \tag{11}$$

where the sample and the noise vectors are given by:

$$\mathbf{y} = \begin{pmatrix} y_1 \\ \vdots \\ y_m \end{pmatrix}, \boldsymbol{\eta} = \begin{pmatrix} \eta_1 \\ \vdots \\ \eta_m \end{pmatrix}.$$

¹ The ℓ_0 -norm of a vector $\mathbf{x} \in \mathbb{C}^n$ is defined by:

$$\|\mathbf{x}\|_0 := \sum_{i=1}^n 1(x_i \neq 0),$$

where $1(\cdot)$ is the identity function. Needless to say that ℓ_0 -norm is called a norm just as a convention. It is, indeed, not a norm.

The noise vector satisfies $\|\boldsymbol{\eta}\|_\infty \leq \epsilon$. The matrix \mathbf{A} , called the measurement or sensing matrix, is given by:

$$\mathbf{A} = \begin{pmatrix} D_0^{0,0}(\theta_1, \phi_1, \chi_1) & \dots & D_{B-1}^{B-1,B-1}(\theta_1, \phi_1, \chi_1) \\ \vdots & & \\ D_0^{0,0}(\theta_m, \phi_m, \chi_m) & \dots & D_{B-1}^{B-1,B-1}(\theta_m, \phi_m, \chi_m) \end{pmatrix}. \quad (12)$$

The columns of \mathbf{A} consists of m different samples of Wigner D-functions, and its rows are comprised of a single sample of all Wigner D-functions of degree less than B . The ordering of Wigner D-functions in a row is arbitrary. The only caveat is that the vector $\mathbf{g} \in \mathbb{C}^N$ of N coefficients should be similarly ordered. For simplicity we assumed that the degree and orders of the Wigner D-function in the column $q \in [N]$ is determined by three functions $l(q)$, $k(q)$ and $n(q)$. In this way, the Wigner D-function of the column q is $D_{l(q)}^{k(q),n(q)}$. The entry q of \mathbf{g} is $\hat{g}_{l(q)}^{k(q),n(q)}$, and the matrix \mathbf{A} is written as

$$\mathbf{A} = [A_{p,q}]_{p \in [m], q \in [N]} : \quad A_{p,q} = D_{l(q)}^{k(q),n(q)}(\theta_p, \phi_p, \chi_p). \quad (13)$$

The linear inverse problem is similarly defined for spherical harmonics by removing the polarization parameter from the above equation. In both cases, we are interested in finding the Fourier coefficients from few samples.

If the vector of coefficients \mathbf{g} , or \mathbf{f} , are sparse or compressible, there are many algorithms for finding the coefficients from a number of samples m that is fewer than the dimension N . In this paper, we use quadratically constrained basis pursuit, i.e., ℓ_1 -minimization problem to solve the problem (11). The focus, however, is more on different sampling patterns and their effectiveness for signal recovery. The quadratically constrained basis pursuit is defined below:

$$\mathbf{g}^\# = \arg \min_{\mathbf{z} \in \mathbb{C}^N} \|\mathbf{z}\|_1 \quad \text{subject to} \quad \|\mathbf{A}\mathbf{z} - \mathbf{y}\|_2 \leq \sqrt{m}\epsilon. \quad (\text{QCBP})$$

In the next sections, we consider various sampling patterns and their recovery guarantees.

3 Sparse Recovery Guarantees for Random Matrices

How should the sensing matrix \mathbf{A} be chosen for the program (QCBP) to find a *good* approximation of compressible coefficients vectors? The error of a good approximation is only bounded by the model and measurement inaccuracies determined by the s -sparse approximation error and the noise strength. Therefore, we are interested in choosing \mathbf{A} such that any s -sparse vector can be perfectly recovered from noiseless linear measurements. This is shown to be possible in compressed sensing literature if the samples are taken randomly from a class of distributions. In most of these results, the proof amounts to showing Restricted Isometry Property, a sufficient condition for signal recovery, for the sensing matrix \mathbf{A} . The RIP is defined below.

Definition 1. A matrix \mathbf{A} satisfies the restricted isometry property of order s with constant $\delta \in (0, 1)$, if the following inequalities hold for all s -sparse vectors \mathbf{x}

$$(1 - \delta) \|\mathbf{x}\|_2^2 \leq \|\mathbf{A}\mathbf{x}\|_2^2 \leq (1 + \delta) \|\mathbf{x}\|_2^2.$$

The smallest number δ , denoted by δ_s , is called the restricted isometry constant of \mathbf{A} .

Fortunately a general result for BOSs is available. The result is used later, and we present it for the paper to be self-contained.

Theorem 1 (RIP for BOS [4, Theorem 12.31]). *Consider a set of bounded orthonormal basis $\psi_q, q \in [N]$ that are orthonormal with respect to a probability measure ν on the measurable space \mathcal{D} . Consider the matrix $\boldsymbol{\psi} \in \mathbb{C}^{m \times N}$ with entries*

$$\psi_{p,q} = \psi_q(t_p), \quad p \in [m], q \in [N]$$

constructed with i.i.d. samples t_p from the measure ν . Suppose that $\sup_{q \in [N]} \|\psi_q\|_\infty \leq K$. If

$$m \gtrsim \delta^{-2} K^2 s \log^3(s) \log(N)$$

then with probability at least $1 - N^{-\gamma \log^3(s)}$, the restricted isometry constant δ_s of $\frac{1}{\sqrt{m}}\boldsymbol{\psi}$ satisfies $\delta_s \leq \delta$ for $\delta \in (0, 1)$. The constants $C, \gamma \geq 0$ are universal.

The crucial assumption, as we will see later, is the uniform boundedness of $\psi_q(\cdot)$. Once the RIP property is satisfied by a matrix, s -sparse vectors are recovered perfectly using the program (QCBP). RIP property, indeed, implies the robust and stable null space property which is the necessary and sufficient condition for unique recovery (see [4, Chapter 12]). The following theorem summarizes this result.

Theorem 2 (Sparse Recovery for RIP Matrices [4, Corollary 12.34]). *Suppose that the matrix $\Psi \in \mathbb{C}^{m \times N}$ has restricted isometry constant $\delta_{2s} \leq 0.4931$. Suppose that the measurements are noisy $\mathbf{y} = \Psi \mathbf{x} + \boldsymbol{\eta}$ with $\|\boldsymbol{\eta}\|_\infty \leq \epsilon$. If $\mathbf{x}^\#$ is the minimizer of*

$$\mathbf{x}^\# = \arg \min \|\mathbf{z}\|_1 \text{ subject to } \|\mathbf{y} - \Psi \mathbf{z}\|_2 \leq \epsilon,$$

then

$$\|\mathbf{x} - \mathbf{x}^\#\|_2 \lesssim C \left(\frac{\sigma_s(\mathbf{x})_1}{\sqrt{s}} + \epsilon \right),$$

where C depends only on δ_{2s} . Without noise, we have $\mathbf{x} = \mathbf{x}^\#$ for s -sparse vectors \mathbf{x} .

Unfortunately the results of Theorem 1 and 2 provide only weak bounds for spherical harmonics and Wigner D-functions, because these orthonormal functions are not uniformly bounded, as mentioned in [9]. More precisely, see that:

$$Y_l^0(0, \phi) = \sqrt{\frac{2l+1}{4\pi}}. \quad (14)$$

The value of $Y_l^0(0, \phi)$ can be shown to be the upper bound on all spherical harmonics of degree l . This means that all spherical harmonics of degree less than B are bounded by $\sqrt{\frac{2B-1}{4\pi}}$, and the bound is tight. Since the ambient dimension N is equal to B^2 , the uniform upper bound K on spherical harmonics depends on N as $K = O(\sqrt{B})$. Theorem 1, then, yields a bound on m that depends on the ambient dimension as $O(\sqrt{N})$. A more general dependence of this type appeared in the paper [10]. This dependence is terrible for large dimensions and very sparse vectors.

Rauhut and Ward in [9] and Burq et al. in [10] used a preconditioning technique that improves this dependence for spherical harmonics. At the core of the preconditioning technique lies the following inequality:

$$\left| (\sin^2 \theta \cos \theta)^{1/6} Y_l^k(\theta, \phi) \right| \lesssim (l+1)^{1/6} \quad (15)$$

Burq et al. [10] change the probability measure defined on \mathbb{S}^2 to the measure $d\nu = |\tan \theta|^{1/3} d\theta d\phi$ and preconditioned the spherical harmonics by $(\sin^2 \theta \cos \theta)^{1/6}$. Note that further normalization by a constant is needed to turn the new measure to a probability measure. The new probability measure, however, improves the dependence of m on N to $O(N^{1/6})$, which improves also the previous preconditioning by $(\sin \theta)^{1/2}$ proposed in [9].

The upper bound on Wigner D-functions, similarly, depends on N . In particular, see from the equality 10, that the upper bound K is also $O(\sqrt{B})$. Since N is related to B by $N = \frac{B(2B-1)(2B+1)}{3}$, the measurement number m should depend on N as $O(N^{1/3})$. We propose a similar preconditioning technique to improve this bound. The following inequality is crucial for our derivations:

$$\left| (\sin \theta)^{1/2} d_l^{k,n}(\cos \theta) \right| \lesssim (2l+1)^{-1/4}.$$

We prove the above inequality in the appendix. This inequality suggests that the upper bound is improved if we precondition $D_l^{k,n}$ by $(\sin \theta)^{1/2}$. The preconditioning technique can be applied with Theorem 1 and Theorem 2 to yield the recovery guarantee for random sampling patterns, stated in the following theorem.

Theorem 3. *Consider the problem (11) of finding Fourier coefficients \mathbf{g} of a band-limited function $g \in L^2(\text{SO}(3))$ from noisy linear measurements $\mathbf{y} = \mathbf{A}\mathbf{g} + \boldsymbol{\eta}$ with $\|\boldsymbol{\eta}\|_\infty \leq \epsilon$.*

Suppose that the sensing matrix \mathbf{A} is constructed as (12) using m i.i.d. samples $(\theta_p, \phi_p, \chi_p)$, $p \in [m]$ drawn uniformly from $[0, \pi] \times [0, 2\pi] \times [0, 2\pi]$. Let \mathbf{P} be a diagonal matrix with $P_{ii} = \sin(\theta_i)^{1/2}$. The number of measurements m is assumed to satisfy the following inequality

$$m \gtrsim N^{1/6} s \log^3(s) \log(N).$$

Then with probability at least $1 - N^{-\gamma \log^3(s)}$, the following holds. If $\mathbf{g}^\#$ is the solution to the following problem

$$\mathbf{g}^\# = \arg \min \|\mathbf{z}\|_1 \text{ subject to } \|\mathbf{P}\mathbf{A}\mathbf{z} - \mathbf{P}\mathbf{y}\|_2 \leq \sqrt{m}\epsilon.$$

then,

$$\|\mathbf{g} - \mathbf{g}^\#\|_2 \lesssim \frac{\sigma_s(\mathbf{g})_1}{\sqrt{s}} + \epsilon.$$

In particular, when the measurements are not noisy, the recovery is unique for s -sparse signal, namely $\mathbf{g} = \mathbf{g}^\#$.

Proof. The proof is given in Appendix A. \square

Remark 2. The role of preconditioning matrix is to counter the increase of Wigner D-functions at the endpoints of the interval. For a compact n -dimensional Riemannian manifold, the first N eigenfunctions are uniformly bounded by $N^{n-1/2n}$ in [10, Corollary 2]. For $\text{SO}(3)$, a 3-dimensional compact manifold, this approach yields the bound $N^{1/3}$ which is worse than the results above. As stated in [10], this bound deteriorates as the dimension of underlying manifold increases. The general results in [7, 10] do not apply here since Wigner D-functions are not defined for surfaces of revolution. In the numerical results, we also consider the performance of preconditioning and measure in [10]. It is, however, not clear at the moment how a similar bound can be obtained for eigenfunctions on $\text{SO}(3)$.

4 Coherence Analysis of Sensing Matrices for Regular Sampling Patterns

Theorem 3 guarantees that random samples are suitable for sparse recovery of sparse Wigner D-expansion, while a similar result for spherical harmonics was given in [9]. Practitioners use, however, more deterministic and regular samples. For instance, the samples in antenna design applications are taken through robotic probes, which have physical limitations for taking too close measurements. Therefore sampling patterns that are sufficiently distant and lead to smoother probe movements are preferred. In practice, the sampling points are chosen from some known structures like equiangular sampling patterns. The main challenge is to find suitable regular patterns for sparse recovery.

Verifying RIP for deterministic sensing matrices is computationally hard. Furthermore, except the single example of [38], only randomly generated sensing matrices have been shown so far to satisfy RIP. There are, however, examples of matrices that do not satisfy RIP and yet provide provable recovery guarantees [39]. Therefore, instead of using RIP, we choose another notion to assess whether a sensing matrix is suitable for solving inverse problems. There are other concepts for evaluating the *goodness* of sensing matrices such as spark or mutual coherence of a matrix. We focus on the notion of mutual coherence in this work.

Definition 2. The mutual coherence of a matrix $\mathbf{A} = [\mathbf{a}_1 \dots \mathbf{a}_N] \in \mathbb{C}^{m \times N}$ is defined as the maximum of the normalized inner product of columns of the matrix, i.e.,

$$\mu(\mathbf{A}) := \max_{1 \leq i < j \leq N} \frac{|\langle \mathbf{a}_i, \mathbf{a}_j \rangle|}{\|\mathbf{a}_i\|_2 \|\mathbf{a}_j\|_2}.$$

The mutual coherence belongs to the interval $[0, 1]$. As a rule of thumb, the coherence of the sensing matrix should be very small for recovery of moderately sparse vectors. It is possible to obtain recovery guarantees for deterministic sensing matrices using its coherence value (for example see [4, Theorem 5.7]). These results, however, yield bounds on the number of measurements that scale quadratically with the sparsity level. This is underwhelming even for moderate sparsity regime. Nevertheless, the coherence can still be used as a good indication for fitness of a sensing matrix, which is the approach we opt in this article.

The mutual coherence expression for spherical harmonics, $\mu_1(\mathbf{A})$, and Wigner D-functions, $\mu_2(\mathbf{A})$, are given by

$$\mu_1(\mathbf{A}) := \max_{1 \leq r < q \leq N} \left| \sum_{p=1}^m \frac{Y_{l(q)}^{k(q)}(\theta_p, \phi_p) \overline{Y_{l(r)}^{k(r)}(\theta_p, \phi_p)}}{\|Y_{l(q)}^{k(q)}(\boldsymbol{\theta}, \boldsymbol{\phi})\|_2 \|Y_{l(r)}^{k(r)}(\boldsymbol{\theta}, \boldsymbol{\phi})\|_2} \right| \quad (16)$$

$$\mu_2(\mathbf{A}) := \max_{1 \leq r < q \leq N} \left| \sum_{p=1}^m \frac{D_{l(q)}^{k(q), n(q)}(\theta_p, \phi_p, \chi_p) \overline{D_{l(r)}^{k(r), n(r)}(\theta_p, \phi_p, \chi_p)}}{\|D_{l(q)}^{k(q), n(q)}(\boldsymbol{\theta}, \boldsymbol{\phi}, \boldsymbol{\chi})\|_2 \|D_{l(r)}^{k(r), n(r)}(\boldsymbol{\theta}, \boldsymbol{\phi}, \boldsymbol{\chi})\|_2} \right|, \quad (17)$$

where we adopt the following convention:

$$\mathbf{Y}_l^k(\boldsymbol{\theta}, \boldsymbol{\phi}) := \begin{pmatrix} Y_l^k(\theta_1, \phi_1) \\ \vdots \\ Y_l^k(\theta_m, \phi_m) \end{pmatrix}$$

and

$$\mathbf{D}_l^{k,n}(\boldsymbol{\theta}, \boldsymbol{\phi}, \boldsymbol{\chi}) := \begin{pmatrix} D_l^{k,n}(\theta_1, \phi_1, \chi_1) \\ \vdots \\ D_l^{k,n}(\theta_m, \phi_m, \chi_m) \end{pmatrix}.$$

As a reminder, the problem of designing sensing matrix for spherical harmonics and Wigner D-expansion boils down to finding the sequence of azimuth, elevation, and for Wigner D-functions case, polarization over which the measurements are taken. For spherical harmonics, the sampling pattern is given by pairs (θ_p, ϕ_p) with $p \in [m]$, $\theta_p \in [0, \pi]$ and $\phi_p \in [0, 2\pi)$. For Wigner D-expansion, a rotation variable should be added and the sampling pattern is given by pairs $(\theta_p, \phi_p, \chi_p)$ with $p \in [m]$, $\theta_p \in [0, \pi]$ and $\phi_p, \chi_p \in [0, 2\pi)$. In the next section, our first result states that many sampling patterns, which are widely used in practice, have high mutual coherence and therefore are terrible for compressed sensing.

4.1 Modularly Symmetric Patterns over Azimuth and Polarization

A large class of regular sampling patterns select their sampling patterns on a regular grid over θ, ϕ and χ . Some of these sampling patterns, however, would lead to high mutual coherence and therefore should be avoided for compressed sensing applications. Spherical harmonics and Wigner D-functions are defined by associated Legendre polynomials and Jacobi polynomials. These polynomials are linearly related to each other for different orders and degrees. Through this relation, two columns of the sensing matrix can become strongly coherent in some cases. The following theorem concerns one of these cases. It states the regular sampling on ϕ and χ can lead to full coherence.

Theorem 4. *Let the matrix $\mathbf{A} \in \mathbb{C}^{m \times N}$ be constructed from samples of spherical harmonics $\mathbf{Y}_l^k(\boldsymbol{\theta}, \boldsymbol{\phi})$ or Wigner D-functions $\mathbf{D}_l^{k,n}(\boldsymbol{\theta}, \boldsymbol{\phi}, \boldsymbol{\chi})$ for a signal with bandwidth B using a sampling pattern that satisfies*

$$\begin{aligned} 2k\phi_i &\equiv 2k\phi_j \pmod{2\pi}, & \forall i, j \in [m] \\ 2n\chi_i + 2k\phi_i &\equiv 2n\chi_j + 2k\phi_j \pmod{2\pi}, & \forall i, j \in [m] \end{aligned}$$

for some $-(B-1) \leq k, n \leq B-1$. Then the mutual coherence of this matrix attains its maximum, i.e., $\mu(\mathbf{A}) = 1$.

Proof. Associated Legendre polynomials satisfy a symmetry relation over order in the following sense [40]:

$$P_l^{-k}(\cos \theta) = (-1)^k C_{lk} P_l^k(\cos \theta) \quad (18)$$

where $C_{lk} = \sqrt{\frac{(l-k)!}{(l+k)!}}$. This relation implies immediately a symmetric relation over orders of spherical harmonics, namely

$$\mathbf{Y}_l^{-k}(\boldsymbol{\theta}, \boldsymbol{\phi}) = (-1)^k \overline{\mathbf{Y}_l^k(\boldsymbol{\theta}, \boldsymbol{\phi})} = (-1)^k \mathbf{Y}_l^k(\boldsymbol{\theta}, \boldsymbol{\phi}) e^{-i2k\phi}. \quad (19)$$

Now if the azimuth sampling points are selected as $2k\phi_i \equiv 2k\phi_j \pmod{2\pi}$ for all $i, j \in [m]$, then the equality $e^{-i2k\phi_i} = e^{-i2k\phi_j}$ holds, which implies:

$$\mathbf{Y}_l^{-k}(\boldsymbol{\theta}, \boldsymbol{\phi}) = C_k \mathbf{Y}_l^k(\boldsymbol{\theta}, \boldsymbol{\phi})$$

for some constant C_k . This means that there are two columns of the matrix, corresponding to these two basis functions, totally coherent with each other and therefore yielding the coherence equal to one. On the other hand, it can be easily seen that by inverting the sign of orders of Wigner D-functions, the orders of respective Jacobi polynomial does not change and therefore:

$$\mathbf{d}_l^{k,n}(\cos \theta) = (-1)^{n-k} \mathbf{d}_l^{-k,-n}(\cos \theta). \quad (20)$$

which means that

$$\begin{aligned} \mathbf{D}_l^{k,n}(\boldsymbol{\theta}, \boldsymbol{\phi}, \boldsymbol{\chi}) &= (-1)^{n-k} \overline{\mathbf{D}_l^{-k,-n}(\boldsymbol{\theta}, \boldsymbol{\phi}, \boldsymbol{\chi})} \\ &= (-1)^{n-k} \mathbf{D}_l^{-k,-n}(\boldsymbol{\theta}, \boldsymbol{\phi}, \boldsymbol{\chi}) e^{-j2k\phi} e^{-j2n\chi}. \end{aligned}$$

If for some k, n , we have $2n\chi_i + 2k\phi_i \equiv 2n\chi_j + 2k\phi_j \pmod{2\pi}$ for all $i, j \in [m]$, then similar to spherical harmonics, it holds that:

$$D_l^{k,n}(\theta, \phi, \chi) = (-1)^{n-k} D_l^{-k,-n}(\theta, \phi, \chi).$$

And therefore there are two columns that are completely coherent and therefore the mutual coherence is equal to one. \square

The previous theorem precludes some of familiar sampling patterns. One notable example is equiangular sampling on ϕ namely, $\phi_p = \frac{2\pi(p-1)}{m-1}$ for $p \in [m]$. If the number of samples are odd and smaller than $2B - 1$, the sensing matrix has the coherence equal to one with columns corresponding to $k = \frac{m-1}{2}$ being completely coherent. For Wigner D-functions, the equiangular samples on the azimuth ϕ and polarization χ are not proper sampling patterns. Note that in Wigner D-functions case, it is possible to end up with full coherence even if the polarization and azimuth angles are chosen irregularly.

Theorem 4 provides a first step to understand what to avoid in sensing matrix designs. In the next sections, we first provide an alternative way of characterizing coherence using tools originally developed in quantum mechanics. Afterwards, instead of imposing regularity on ϕ and χ , we study regular sampling on the elevation θ .

4.2 Coherence Analysis using Wigner 3j Symbols

Spherical harmonics and Wigner D-functions express wave functions in the study of angular momentum in quantum mechanics. Their products appear in the characterization of total angular momenta of a composite system in terms of the angular momentum of its two sub-systems. This characterization involves a decomposition of the wave function into two wave functions with different angular momenta. The coefficients of this decomposition are given by the Clebsch-Gordan coefficients, also known as Wigner or vector coupling coefficients, as well as Wigner 3j symbols [37,41–44]. We focus on the latter and provide briefly some of the useful identities here. Wigner 3j symbols are denoted by $\begin{pmatrix} l_1 & l_2 & l_3 \\ n_1 & n_2 & n_3 \end{pmatrix}$, and their exact formula is given in [36, Section 7.10.2] or [43]. Despite their complex expressions, Wigner 3j symbols have a few useful properties. The so-called *selection rules* state that Wigner 3j symbols $\begin{pmatrix} l_1 & l_2 & l_3 \\ k_1 & k_3 & k_3 \end{pmatrix}$ are non-zero only if:

- The absolute value of k_i does not exceed l_i , i.e., $-l_i \leq k_i \leq l_i$ for $i = 1, 2, 3$
- The summation of all k_i should be zero: $k_1 + k_2 + k_3 = 0$.
- Triangle inequality holds for l_i 's: $|l_1 - l_2| \leq l_3 \leq l_1 + l_2$.
- The sum of all l_i 's should be an integer $l_1 + l_2 + l_3 \in \mathbb{N}$.
- If $k_1 = k_2 = k_3 = 0$, $l_1 + l_2 + l_3 \in \mathbb{N}$ should be an even integer.

If one of the above conditions does not hold, the corresponding Wigner 3j symbol will be zero.

In coherence analysis of the sensing matrix in (17) and (16), one encounters sums over products of spherical harmonics or Wigner D-functions. We can use Wigner 3j symbols to express these sums in terms of sum of spherical harmonics, or respectively Wigner D-functions. The decomposition reveals in another way the effect of sampling patterns on the mutual coherence. The following proposition, derived from the decomposition based on Wigner 3j symbols, characterizes the inner product between two columns of the sensing matrix.

Proposition 1. *Let $D_l^{k,n}(\theta, \phi, \chi)$ be the Wigner D-function with degree l and orders k, n , and let $Y_l^k(\theta, \phi)$ be the spherical harmonics with degree l and order k . Then the following identities hold:*

$$\begin{aligned} & \sum_{p=1}^m \overline{D_{l_1}^{k_1,n_1}(\theta_p, \phi_p, \chi_p)} D_{l_2}^{k_2,n_2}(\theta_p, \phi_p, \chi_p) \\ &= C_{k_2,n_2} \sum_{\hat{l}=|l_2-l_1|}^{l_1+l_2} (2\hat{l}+1) \begin{pmatrix} l_1 & l_2 & \hat{l} \\ -n_1 & n_2 & -\hat{n} \end{pmatrix} \begin{pmatrix} l_1 & l_2 & \hat{l} \\ -k_1 & k_2 & -\hat{k} \end{pmatrix} \left(\sum_{p=1}^m D_{\hat{l}}^{\hat{k},\hat{n}}(\theta_p, \phi_p, \chi_p) \right), \end{aligned} \quad (21)$$

$$\begin{aligned}
\sum_{p=1}^m \overline{Y_{l_1}^{k_1}(\theta_p, \phi_p)} Y_{l_2}^{k_2}(\theta_p, \phi_p) &= (-1)^{k_1} Y_{l_1}^{-k_1}(\theta_p, \phi_p) Y_{l_2}^{k_2}(\theta_p, \phi_p) \\
&= (-1)^{k_2} \sum_{\hat{l}=|l_1-l_2|}^{l_1+l_2} \sqrt{\frac{(2l_1+1)(2l_2+1)(2\hat{l}+1)}{4\pi}} \begin{pmatrix} l_1 & l_2 & \hat{l} \\ 0 & 0 & 0 \end{pmatrix} \begin{pmatrix} l_1 & l_2 & \hat{l} \\ -k_1 & k_2 & -\hat{k} \end{pmatrix} \left(\sum_{p=1}^m Y_{\hat{l}}^{\hat{k}}(\theta_p, \phi_p) \right).
\end{aligned} \tag{22}$$

where $\hat{k} = k_2 - k_1$ and $\hat{n} = n_2 - n_1$ and the phase factor $C_{k_2, n_2} = (-1)^{k_2+n_2}$.

Proof. The product of two Wigner D-functions of degrees l_1 and l_2 and orders k_1, n_1 and k_2, n_2 writes in terms of the Wigner 3j symbols as

$$D_{l_1}^{k_1, n_1}(\theta, \phi, \chi) D_{l_2}^{k_2, n_2}(\theta, \phi, \chi) = \sum_{\hat{l}=|l_1-l_2|}^{l_1+l_2} (2\hat{l}+1) \begin{pmatrix} l_1 & l_2 & \hat{l} \\ k_1 & k_2 & -\hat{k} \end{pmatrix} \begin{pmatrix} l_1 & l_2 & \hat{l} \\ n_1 & n_2 & -\hat{n} \end{pmatrix} (-1)^{\hat{k}+\hat{n}} D_{\hat{l}}^{\hat{k}, \hat{n}}(\theta, \phi, \chi), \tag{23}$$

where $\hat{n} = n_1 + n_2$ and $\hat{k} = k_1 + k_2$ [43, pp. 61-62]. The spherical harmonics version of the expansion can be obtained by using $n_1 = n_2 = 0$.

From the conjugate property of these functions, we know that $\overline{D_{l_1}^{k_1, n_1}(\theta, \phi, \chi)} = (-1)^{k_1-n_1} D_{l_1}^{-k_1, -n_1}(\theta, \phi, \chi)$ and $\overline{Y_{l_1}^{k_1}(\theta, \phi)} = (-1)^{k_1} Y_{l_1}^{-k_1}(\theta, \phi)$. The proof follows with standard manipulations by plugging in these identities to (23). \square

According to Proposition 1, the inner product between columns of the sensing matrix depends on the sampling pattern through the sum $\sum_{p=1}^m Y_{\hat{l}}^{\hat{k}}(\theta_p, \phi_p)$ or $\sum_{p=1}^m D_{\hat{l}}^{\hat{k}, \hat{n}}(\theta_p, \phi_p, \chi_p)$. The next theorem uses this characterization when the elevation samples are chosen symmetrically in the following sense.

Definition 3 (Cosine-symmetric sampling). Cosine-symmetric sampling patterns are defined by a set of m samples $(\theta_p, \phi_p, \chi_p)$ for $p = 1, \dots, m$ such that the set $\{\cos \theta_1, \dots, \cos \theta_m\}$ consists of symmetric points around the origin inside $[-1, 1]$.

Theorem 5. Suppose that m samples are chosen such that the elevation samples $\theta_1, \dots, \theta_m$ are cosine-symmetric. Consider two columns of the sensing matrix corresponding to samples of two spherical harmonics with equal order $k_1 = k_2$ and different degrees l_1 and l_2 . If $l_1 + l_2$ is odd, then the columns are orthogonal. The same conclusion holds for two Wigner D-functions when one pair of orders are equal and the other pair of orders are equal to zero.

Proof. We start with spherical harmonics. We use Proposition 1. Note that:

$$\begin{aligned}
D_l^{0,0}(\theta_p, \phi_p, \chi_p) &= \frac{1}{2\pi} Y_l^0(\theta_p, \phi_p) = \sqrt{\frac{2l+1}{8\pi^2}} P_l^0(\cos \theta_p) \\
&= \sqrt{\frac{2l+1}{8\pi^2}} P_l(\cos \theta_p),
\end{aligned}$$

where $P_l(\cos \theta)$ is the Legendre polynomial. Legendre polynomials are odd functions for odd l . This means that for the cosine-symmetric elevation sampling, when l is odd, it holds that:

$$\sum_{p=1}^m P_l(\cos \theta_p) = 0.$$

Therefore Proposition 1 implies that:

$$\begin{aligned}
\sum_{p=1}^m \overline{Y_{l_1}^k(\theta_p, \phi_p)} Y_{l_2}^k(\theta_p, \phi_p) &= \\
(-1)^k \sum_{\hat{l}=|l_1-l_2|, \text{even}}^{l_1+l_2} \sqrt{\frac{(2l_1+1)(2l_2+1)(2\hat{l}+1)}{4\pi}} \begin{pmatrix} l_1 & l_2 & \hat{l} \\ 0 & 0 & 0 \end{pmatrix} \begin{pmatrix} l_1 & l_2 & \hat{l} \\ -k & k & 0 \end{pmatrix} \left(\sum_{p=1}^m Y_{\hat{l}}^0(\theta_p, \phi_p) \right).
\end{aligned} \tag{24}$$

On the other hand, according to the selection rules, if $l_1 + l_2$ is odd and \hat{l} is even, then $\begin{pmatrix} l_1 & l_2 & \hat{l} \\ 0 & 0 & 0 \end{pmatrix} = 0$, which proves the theorem. A similar argument works for the Wigner D-functions. \square

Theorem 5 implies that, if the elevation sampling pattern is cosine-symmetric, there are at least $\lfloor \frac{B}{2} \rfloor$ columns that are mutually orthogonal. Cosine-symmetric sampling patterns are also regular, hence, suitable for practical measurements. Using this insight, in the next section, we propose a cosine-symmetric pattern with minimal coherence.

5 Equispaced Elevation Sampling for Spherical Harmonics and Wigner D-Functions

As we discussed, among regular sampling patterns, equiangular sampling patterns on azimuth and polarization lead to coherent, and therefore undesirable, sensing matrices. On the other hand, a class of regular sampling patterns on the elevation yield incoherent measurements as in Theorem 5.

As soon as the elevation sampling is fixed, the mutual coherence is automatically bounded from below regardless of the choice of azimuth sampling patterns. This is because, in the inner products of columns with equal orders $k_1 = k_2 = k$ and $n_1 = n_2 = n$, the terms $e^{ik_1\phi_p}$ and $e^{-ik_2\phi_p}$ and the terms $e^{in_1\chi_p}$ and $e^{-in_2\chi_p}$ cancel each other out. Furthermore the ℓ_2 -norm of $Y_l^k(\boldsymbol{\theta}, \boldsymbol{\phi})$ and $D_l^{k,n}(\boldsymbol{\theta}, \boldsymbol{\phi}, \boldsymbol{\chi})$ depends only on elevation sampling for all degrees and orders. We state this simple result in the following proposition.

Proposition 2. *Let the elevation sampling be fixed to $\theta_1, \theta_2, \dots, \theta_m$. For all possible choices of azimuth ϕ_p , and polarization χ_p , $p \in [m]$, it holds that*

$$\begin{aligned}\mu_1(\mathbf{A}) &\geq \max_{\substack{l \neq r \\ |k| \leq \min(l, r)}} \frac{\left| \sum_{p=1}^m P_l^k(\cos \theta_p) P_r^k(\cos \theta_p) \right|}{\|P_l^k(\cos \boldsymbol{\theta})\|_2 \|P_r^k(\cos \boldsymbol{\theta})\|_2}, \\ \mu_2(\mathbf{A}) &\geq \max_{\substack{l \neq r \\ |k|, |n| \leq \min(l, r)}} \frac{\left| \sum_{p=1}^m d_l^{k,n}(\cos \theta_p) d_r^{k,n}(\cos \theta_p) \right|}{\|d_l^{k,n}(\cos \boldsymbol{\theta})\|_2 \|d_r^{k,n}(\cos \boldsymbol{\theta})\|_2},\end{aligned}$$

where

$$\begin{aligned}P_l^k(\cos \boldsymbol{\theta}) &:= (P_l^k(\cos \theta_1), \dots, P_l^k(\cos \theta_m))^T \\ d_l^{k,n}(\cos \boldsymbol{\theta}) &:= (d_l^{k,n}(\cos \theta_1), \dots, d_l^{k,n}(\cos \theta_m))^T.\end{aligned}$$

In particular it holds that

$$\min \{\mu_1(\mathbf{A}), \mu_2(\mathbf{A})\} \geq \frac{\left| \sum_{p=1}^m P_{B-1}(\cos \theta_p) P_{B-3}(\cos \theta_p) \right|}{\|P_{B-1}(\cos \boldsymbol{\theta})\|_2 \|P_{B-3}(\cos \boldsymbol{\theta})\|_2}$$

where $P_l(\cos \theta)$ is the Legendre polynomial of degree l and

$$P_l(\cos \boldsymbol{\theta}) := (P_l(\cos \theta_1), \dots, P_l(\cos \theta_m))^T.$$

The proposition follows by choosing equal orders in the definition of the coherence. Its lower bounds hold in general for any sampling pattern. Note that Theorem 5 implies that:

$$\sum_{p=1}^m P_{B-1}(\cos \theta_p) P_{B-2}(\cos \theta_p) = 0.$$

This is why the lower bound involves only Legendre polynomials of degree $B-1$ and $B-3$.

On the face of it, Proposition 2 seems trivial. It indicates the sensitivity of mutual coherence to the choice of elevation sampling alone. The lower bound, however, is almost tight for a class of regular sampling patterns on elevation defined below if m is sufficiently large.

Definition 4 (Equispaced Elevation Sampling). The equispaced elevation sampling pattern is defined by the elevation samples θ_p for $p \in [m]$ given by

$$\cos \theta_p = \frac{2p - m - 1}{m - 1},$$

which satisfies $-1 = \cos \theta_1 < \cos \theta_2 < \dots < \cos \theta_{m-2} < \cos \theta_{m-1} < \cos \theta_m = 1$.

For the equispaced elevation sampling, for sufficiently large m , the dominant inner product among all the inner products between the spherical harmonics of equal orders is the inner product between degrees of $B - 1$ and $B - 3$. This can be clearly seen in Fig. 1. After a certain measurement number m , the inner products between columns of equal orders are completely ordered. The ordering of inner products between two columns, say of degree l_1 and l_2 , corresponds to a partial order defined on the degree pairs (l_1, l_2) . This can formally proven. We relegate, however, the detailed derivations of this result to another work [45]. The lower bound is therefore tight in the following sense. Once the elevation sampling pattern is equispaced, there is a fundamental lower bound on the coherence independent of the choice of azimuth and polarization. This lower bound is given in Proposition 2 for sufficiently large m . Note that the number of measurements m should be of $O(N^{1/2})$ for the tightness of the lower bound in this sense. This dependence on N is in general undesirable and cannot be removed, as it can be seen in the numerical result. The exact inequality, however, involves large constants, so that, for many N 's of practical interest, the number of required measurements for the tightness of the lower bound are small. For example, when $N = 1024$, Figure 1 show that after 100 measurements, the lower bound becomes tight. In the next section, we provide a way to choose azimuth sampling patterns that achieves the lower bound for spherical harmonics.

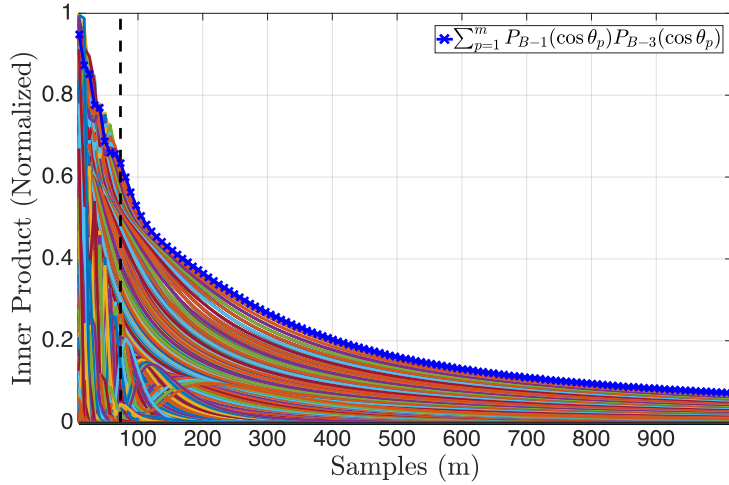


Figure 1: The inner product of two columns of the sensing matrix for different measurement numbers m for $B = 32$ ($N = 1024$)

5.1 Sampling Pattern Design using Coherence Minimization

Is the lower bound of Proposition 2 tight for equispaced sampling patterns? That is, can we find an azimuth sampling pattern that achieves the bound? To do so, we directly minimize the mutual coherence as a figure of merit. The problem of minimizing the mutual coherence for spherical harmonics and Wigner D-functions is non-convex in general since Legendre polynomials, Jacobi polynomials and trigonometric polynomials $e^{i(k^{(r)} - k^{(q)})\phi_p}$ are non-convex. We provide, however, a pattern search algorithm for minimizing the mutual coherence [46]. Pattern search, however, requires less computation time and provides better results in comparison. It is particularly useful as it does not need to calculate the gradient during optimization process. There is, however, no guarantee that the method will converge to the global optimum. See for example [47] for a discussion on the convergence of this algorithm. Although the method has rooms for improvements, it still yields, as we will see, sufficiently good sampling patterns.

First consider spherical harmonics. The algorithm is described in Algorithm 1. It starts by choosing initial ϕ_0 drawn uniformly at random on the interval $[0, 2\pi)^m$. The elevation sampling pattern θ is fixed.

The algorithm has two hyperparameters λ and Δ_0 . The parameter Δ_0 is the initial update step, and determines the search space, which is spanned along the canonical bases. The update step is decreased iteratively by the decay parameter λ . The algorithm tries to find the minimum coherence and its minimizer by checking the neighbor vectors where the initial update step is given as Δ_0 . The mutual coherence at the iteration k is denoted by $\mu(\theta, \phi_k)$. If the search fails, the step size is decreased by scaling with λ . The algorithm stops when the number of iteration is achieved a pre-determined maximum or

when the difference between the update coherence and the lower bound of Proposition 2, denoted by μ_{LB} , is small $|\mu(\theta, \phi_k) - \mu_{LB}| \leq \epsilon$.

Algorithm 1 Pattern search

Initialization : θ given, $\phi_0 \in \mathbb{R}^m$ as initial points, $\Delta_0 > 0$ as initial update step, standard basis e_i for $i \in [m]$, $\lambda \in (0, 1)$
for $k = 0, 1, \dots, k_{\max}$ **until** $|\mu(\theta, \phi_k) - \mu_{LB}| \leq \epsilon$ **do**
 if $\mu(\theta, x) < \mu(\theta, \phi_k)$ for $x \in S_k := \{\phi_k \pm \Delta_k e_i\}$ **then**
 $\phi_{k+1} = x \bmod 2\pi$
 $\Delta_{k+1} = \Delta_k$
 else
 $\phi_{k+1} = \phi_k \bmod 2\pi$
 $\Delta_{k+1} = \lambda \Delta_k$
 end if
end for

Figure 2 compares the mutual coherence of the resulting sampling pattern from Algorithm 1 with other sampling patterns widely used in applications. We use spiral [48], Hammersley [49], Fibonacci [50] and equiangular sampling patterns. The bandwidth of spherical harmonics is chosen as $B = 10$, which yields $N = B^2 = 100$. We plot also the Welch bound, which is the strict lower bound on the coherence of any $m \times N$ matrix. Figure 2, interestingly, shows that the obtained sampling pattern achieves the lower bound of Proposition 2 and outperforms with a large margin the other sampling patterns. We have numerically observed that the lower bound can be achieved using our sampling patterns for N up to 1024. Figure 3 shows the distribution of this sampling points on the sphere for different number of samples m , $B = 32$ and $N = B^2 = 1024$.

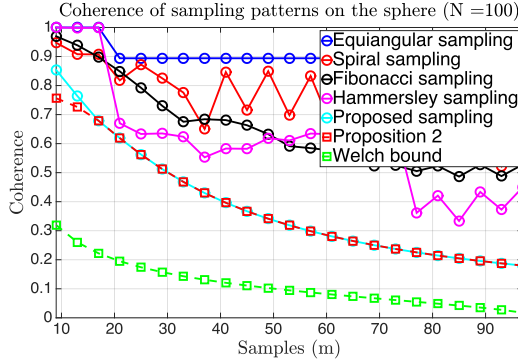


Figure 2: The mutual coherence for different sampling patterns on sphere

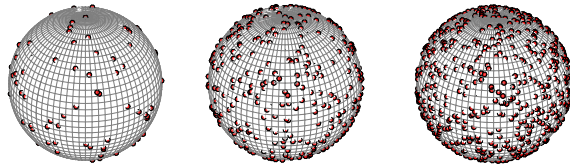


Figure 3: Proposed sampling points ($m=100, m=500, m=900$)

Algorithm 1 can be extended to find pairs of (ϕ_p, χ_p) , $p \in [m]$, for Wigner D-functions. At each step, the algorithm searches simultaneously over the neighbor pairs, and advances similarly by updating Δ_k and ϕ_k, χ_k . The mutual coherence of the resulting sampling pattern is shown in Figure 4 and is compared with other sampling patterns. The bandwidth is chosen as $B = 4$, hence, $N = \frac{B(2B-1)(2B+1)}{3} = 84$. It can be seen that the lower bound of Proposition 2 does not improve on the Welch bound for Wigner D-functions. Although the resulting sampling pattern outperforms significantly the other sampling patterns, it does not achieve the lower bound. This might be an artifact of our optimization method.

A concern about our pattern search algorithm is computational complexity. For $N = 49$ and $N = 100$ and the error tolerance of $|\mu(\theta, \phi_k) - \mu_{LB}| \leq \epsilon = 10^{-4}$, the computation time of the algorithm is shown in Figure 5. When we double the dimension of the signal, it is apparent that the computation time to achieve the same error tolerance would increase approximately fivefold.

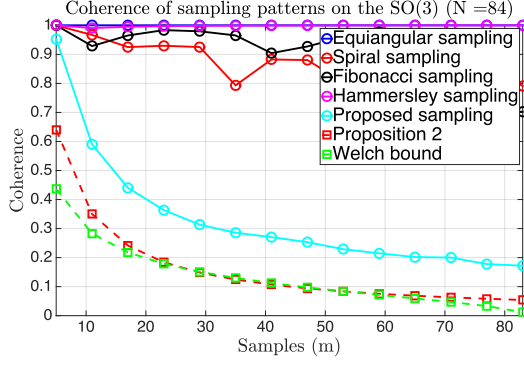


Figure 4: The mutual coherence for different sampling patterns on $SO(3)$

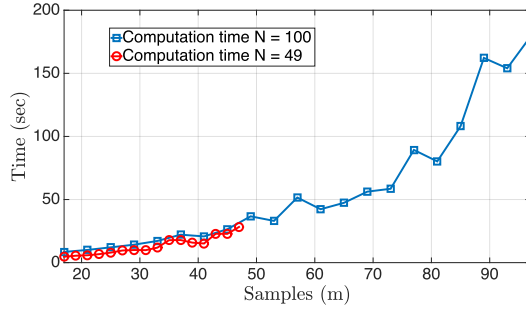


Figure 5: Computation time of algorithm 1

6 Experimental Results

In the previous section, we designed two equispaced sampling patterns, one for the sphere and one for the rotation group with better mutual coherence. In this section, we see if this superiority is translated to the sparse recovery performance as well. Besides, the performance of our proposed sampling patterns is compared with random sampling patterns, which are provably good with high probability for sparse recovery. Two random sampling patterns are considered. The first one is proposed in [9] with the uniform measure, i.e., $d\nu = d\theta d\phi$ for S^2 and $d\nu = d\theta d\phi d\chi$ for $SO(3)$. The second one is given in [10] with the measure $d\nu = |\tan \theta|^{1/3} d\theta d\phi$ for S^2 and $d\nu = |\tan \theta|^{1/3} d\theta d\phi d\chi$ for $SO(3)$.

6.1 Phase transition diagrams

Consider the span of band-limited spherical harmonics with $B = 10$, that is $N = B^2 = 100$. We use the equispaced sampling pattern with θ_p as $\cos \theta_p = \frac{2p-m-1}{m-1}$, $p \in [m]$, and the azimuth samples ϕ_p chosen from Algorithm 1. We solve the linear inverse problem without additive noise using the l_1 -norm minimization package YALL1 [51]. The phase transition diagram of our proposed sampling pattern is plotted with 50 trials and error threshold 10^{-3} . Figure 6 compares the recovery performance of the proposed sampling pattern with several well-known sampling patterns on the sphere and, as well, random sampling. Not only our proposed sampling gives better recovery performance compared with many regular sampling patterns, it even gives a slightly better sparse recovery performance compared with the two random sampling patterns.

A similar result is observed for Wigner D-functions. We consider band-limited functions with $B = 4$ and $N = \frac{B(2B-1)(2B+1)}{3} = 84$. Figure 7 shows the phase transition for the l_1 -minimization. Although our proposed sampling pattern for Wigner D-functions does not achieve the lower bound, it still outperforms other regular sampling patterns, and even slightly random sampling patterns.

6.2 Spherical near-field antenna measurements

One of the main applications of sparse recovery on S^2 and $SO(3)$ is spherical near-field antenna measurement [52]. The expression of electromagnetic field of the antenna using Wigner D-basis coefficients

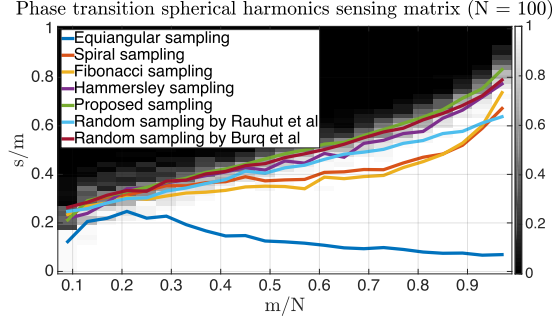


Figure 6: Phase transition diagram of different sampling patterns on the sphere

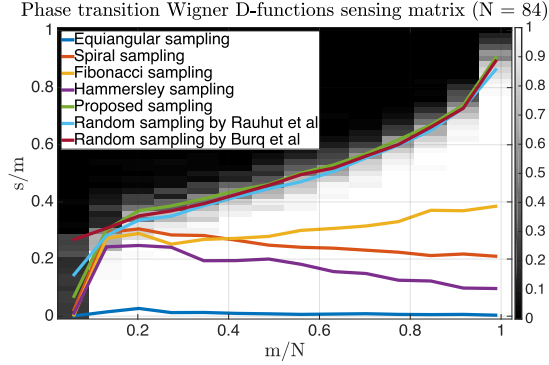


Figure 7: Phase transition diagram of different sampling patterns on the rotation group

is described as follows

$$y(\theta, \phi, \chi) = v \sum_{n=-v_{max}}^{v_{max}} \sum_{h=1}^2 \sum_{l=1}^B \sum_{k=-l}^l T_{hlk} D_l^{k,n}(\theta, \phi, \chi) \quad (25)$$

where $y(\theta, \phi, \chi)$ is a band-limited near-field signal with Wigner D-functions as basis, h denotes the both transverse electric (TE) and magnetic (TM), n and χ denote order and angle to measure polarization, respectively. The bandwidth B is obtained by calculating the wavenumber k and minimum sphere that could cover the whole antenna with radius r_0 . The bandwidth is given by $B = kr_0 + 10$, where the factor 10 is usually added as a correction factor. Normally, it is desirable to measure co- and cross-polarization of the antenna and to use $n = \pm 1$, with angle $\chi \in \{0, \pi/2\}$. The goal is to estimate the spherical wave coefficients of the antenna under test, i.e., T_{hlk} in near-field measurements and use it to determine far-field patterns. The classical method [52] uses Fourier analysis with equiangular samples

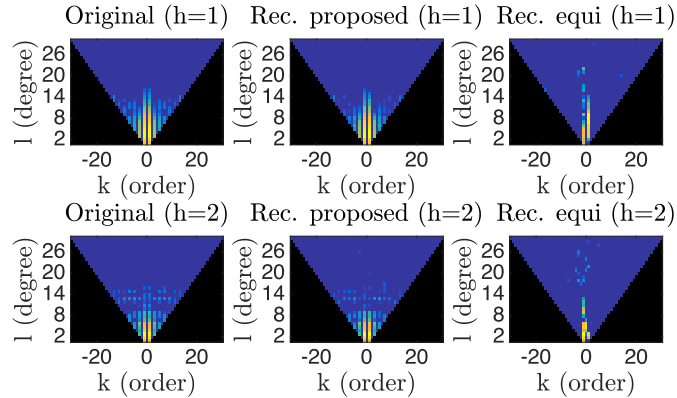


Figure 8: The original spherical wave coefficients compared with basis pursuit recovered coefficients from our proposed sampling pattern and the equiangular sampling pattern

to get the spherical wave coefficient T_{hlk} and lacks the freedom to choose different sampling patterns.

In the real measurement systems, the measurement time directly scales with the number of required samples. In the classical method, we have to take $m \geq 2(B+1)(2B+1)$. The spherical wave coefficients,

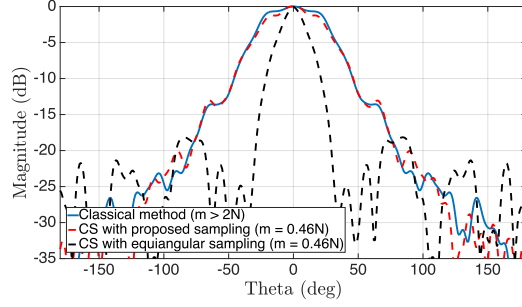


Figure 9: Far-field pattern antenna horn SAS-571 ϕ -cut = 180° and $\chi = 0^\circ$

however, are sparse with respect to Wigner D-basis, which calls for compressed sensing methods. It can be seen in Figure 8 that the important spherical wave coefficients, which is represented by the high intensity of the amplitude, are compressible. In order to get better understanding of spherical near-field measurements we refer to [52, 53]. Figure 8 shows the estimation of spherical wave coefficients by using basis pursuit for antenna horn SAS-571. The bandwidth in this case is given by $B = 30$, which means $N = 960$. Note that the number of coefficients are twice this number, namely 1920, because of the TE/TM coefficient h . It can be seen that the proposed sampling manages to recover same spherical wave coefficients as the conventional method with smaller number of measurements, namely $m = 900$. As it has been shown in [54], our proposed sampling pattern can be used to obtain a smooth trajectory for robotic measurements over the sphere.

The equiangular sampling pattern fails to estimate the spherical wave coefficients. This can be seen as well in far-field signal reconstructions. Figure 9 and Figure 10 show this for polarization $\chi = 0^\circ$ and $\chi = 90^\circ$, respectively. It is assumed that the classical method gives a very good approximation of the ground truth. In comparison, our sampling patterns matches closely the output of the classical method while the equiangular sampling pattern fails to reconstruct the far-field.

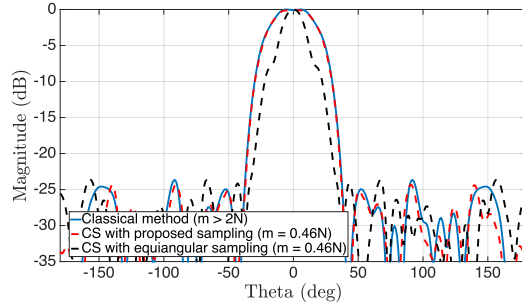


Figure 10: Far-field pattern antenna horn SAS-571 ϕ -cut = 90° and $\chi = 90^\circ$

7 Conclusion and Future Works

How can we find a sampling pattern on the sphere and the rotation group that is also suitable for compressed sensing of signals? By proving RIP property, we show that, as it is expected, random sampling patterns can provably be used for signal recovery on the rotation group. Given the interest in regular sampling patterns in many applications, we consider various existing regular patterns as well. Interestingly, many patterns with symmetric structure on azimuth and polarization suffer from high mutual coherence and are essentially unsuitable for compressed sensing. Instead, we propose a new sampling pattern that imposes regularity on elevation. Using tools from angular momentum analysis in quantum mechanics, we show how appropriate elevation sampling patterns can yield mutually incoherent measurements. But once the elevation sampling is fixed, the mutual coherence is automatically lower bounded, and the best we can do is to choose azimuth and polarization to match this lower bound. We show that this is indeed possible for the sphere using a simple coherence minimization algorithm. The

phase transition diagrams show that our proposed sampling patterns outperform other regular patterns and surpass even random sampling patterns. This work is an attempt for designing deterministic sampling patterns. It is, however, a gap between coherence-based recovery guarantees and RIP-based, as well as other random sampling, guarantees. There are still many open and challenging questions in this context. One promising path is to use number theoretic construction of [38] for \mathbb{S}^2 and $\text{SO}(3)$, and compare it with the proposed sampling patterns.

A Proof of Theorem 3

We have seen that Wigner d-functions are indeed weighted Jacobi polynomials. An upper bound on general weighted orthonormal functions is discussed in [7, Theorem 6.1] and also in [8]. However, we use directly the upper bound on Wigner d-functions obtained in [55, Theorem 1.1].

Lemma 1 (Bound for Jacobi polynomials Wigner d-functions [55]). *For Jacobi polynomials $P_\alpha^{(\xi, \lambda)}$ of degree α and of order (ξ, λ) , there exists a constant $C \geq 0$ such that:*

$$\begin{aligned} \left| (\sin \theta)^{1/2} \sqrt{\gamma} \sin^\xi \left(\frac{\theta}{2} \right) \cos^\lambda \left(\frac{\theta}{2} \right) P_\alpha^{(\xi, \lambda)}(\cos \theta) \right| \\ \leq C(2\alpha + \xi + \lambda + 1)^{-1/4}. \end{aligned} \quad (26)$$

Corollary 1 (Bound for Wigner d-functions). *For Wigner d-functions $d_l^{k,n}(\cos \theta)$, there exists a constant $C \geq 0$ such that $\left| (\sin \theta)^{1/2} d_l^{k,n}(\cos \theta) \right| \leq C(2l + 1)^{-1/4}$.*

The previous corollary is easily obtained using $\xi, \lambda \geq 0$ defined as in Definition 5 and observing that $2\alpha + \xi + \lambda$ equals $2l$. We will later use this corollary to find an upper bound on weighted Wigner D-functions. Since Wigner D-functions are orthonormal, it suffices to find a useful upper bound K on them and then using it in Theorem 1. The following proposition serves this purpose.

Proposition 3 (Bounds on preconditioned Wigner D-functions). *The Wigner D-functions $D_l^{k,n}(\theta, \phi, \chi)$ preconditioned with $(\sin \theta)^{1/2}$ are an orthonormal basis with respect to the product measure $d\nu = d\theta d\phi d\chi$ and satisfy the following upper bound:*

$$\sup_{\substack{0 \leq l \leq B-1 \\ k, n \in \{-l, \dots, l\}}} \left\| (\sin \theta)^{1/2} D_l^{k,n}(\theta, \phi, \chi) \right\|_\infty \leq C_0 N^{\frac{1}{12}},$$

where N is the total number of Wigner D-functions of degree less than B .

Proof. Using Corollary 1, we can see that :

$$\begin{aligned} \left\| (\sin \theta)^{1/2} N_l D_l^{k,n}(\theta, \phi, \chi) \right\|_\infty &= \left\| (\sin \theta)^{1/2} N_l d_l^{k,n}(\cos \theta) \right\|_\infty \\ &\leq C N_l (2l + 1)^{-1/4} = \frac{C}{\sqrt{8\pi^2}} (2l + 1)^{1/4} \\ &\leq \frac{C}{\sqrt{8\pi^2}} (2B - 1)^{1/4} \end{aligned}$$

Note that the number of all orthonormal basis functions N is related B by $N = \frac{B(2B-1)(2B+1)}{3}$. Using the inequality $(2B - 1)^3 \leq 6N$, we have for some constant C_0 :

$$\left\| (\sin \theta)^{1/2} N_l D_l^{k,n}(\theta, \phi, \chi) \right\|_\infty \leq \frac{C}{\sqrt{8\pi^2}} (6N)^{1/12} = C_0 N^{1/12}.$$

□

From Proposition 3, we can use Theorem 1 and 2 to prove sparse recovery guarantees for the coefficients of Wigner D-expansion using random samples of the function. Consider the functions $\varphi_l^{k,n}(\theta, \phi, \chi) = P(\theta) D_l^{k,n}(\theta, \phi, \chi)$, with product measure $d\nu$. Note that the product measure $d\nu = d\theta d\phi d\chi$

with preconditioning function $P(\theta)^2 = \sin(\theta)$ yields the uniform measure. Orthonormality can then be checked easily:

$$\begin{aligned} \int_{\text{SO}(3)} \varphi_l^{k,n}(\theta, \phi, \chi) \overline{\varphi_{l'}^{k',n'}(\theta, \phi, \chi)} d\nu = \\ \int_{\text{SO}(3)} D_l^{k,n}(\theta, \phi, \chi) \overline{D_{l'}^{k',n'}(\theta, \phi, \chi)} \sin(\theta) d\theta d\phi d\chi = \delta_{nn'} \delta_{kk'} \delta_{ll'}. \end{aligned}$$

Therefore the functions $\varphi_l^{k,n}(\theta, \phi, \chi)$ form an orthonormal basis with the upper bound provided in the Proposition 3. Using these with Theorem 1 and 2 finishes the proof.

References

- [1] E. J. Candes and T. Tao, “Decoding by linear programming,” *IEEE Transactions on Information Theory*, vol. 51, no. 12, pp. 4203–4215, 2005.
- [2] E. J. Candès, J. Romberg, and T. Tao, “Robust uncertainty principles: Exact signal reconstruction from highly incomplete frequency information,” *IEEE Transactions on Information Theory*, vol. 52, no. 2, pp. 489–509, 2006.
- [3] E. J. Candes and T. Tao, “Near-Optimal Signal Recovery From Random Projections: Universal Encoding Strategies?” *IEEE Transactions on Information Theory*, vol. 52, no. 12, pp. 5406–5425, Dec. 2006.
- [4] S. Foucart and H. Rauhut, *A mathematical introduction to compressive sensing*. Springer, 2013.
- [5] M. Rudelson and R. Vershynin, “On sparse reconstruction from Fourier and Gaussian measurements,” *Communications on Pure and Applied Mathematics*, vol. 61, no. 8, pp. 1025–1045, Aug. 2008.
- [6] H. Rauhut, “Random sampling of sparse trigonometric polynomials,” *Applied and Computational Harmonic Analysis*, vol. 22, no. 1, pp. 16–42, 2007.
- [7] H. Rauhut and R. Ward, “Sparse Legendre expansions via ℓ_1 -minimization,” *Journal of approximation theory*, vol. 164, no. 5, pp. 517–533, 2012.
- [8] G. Szegő, *Orthogonal polynomials*. American Mathematical Soc., 1939, vol. 23.
- [9] H. Rauhut and R. Ward, “Sparse recovery for spherical harmonic expansions,” *arXiv preprint arXiv:1102.4097*, 2011.
- [10] N. Burq, S. Dyatlov, R. Ward, and M. Zworski, “Weighted eigenfunction estimates with applications to compressed sensing,” *SIAM Journal on Mathematical Analysis*, vol. 44, no. 5, pp. 3481–3501, 2012.
- [11] R. Cornelius, D. Heberling, N. Koep, A. Behboodi, and R. Mathar, “Compressed sensing applied to spherical near-field to far-field transformation,” in *10th European Conference on Antennas and Propagation (EuCAP 2016)*, Davos, Switzerland, April 2016.
- [12] E. Thébault, C. C. Finlay, C. D. Beggan, P. Alken, J. Aubert, O. Barrois, F. Bertrand, T. Bondar, A. Boness, L. Brocco *et al.*, “International geomagnetic reference field: the 12th generation,” *Earth, Planets and Space*, vol. 67, no. 1, p. 79, 2015.
- [13] B. Rafaely, “Analysis and design of spherical microphone arrays,” *IEEE Transactions on Speech and Audio Processing*, vol. 13, no. 1, pp. 135–143, Jan. 2005.
- [14] N. Jarosik, C. L. Bennett, J. Dunkley, B. Gold, M. R. Greason, M. Halpern, R. S. Hill, G. Hinshaw, A. Kogut, E. Komatsu, D. Larson, M. Limon, S. S. Meyer, M. R. Nolte, N. Odegard, L. Page, K. M. Smith, D. N. Spergel, G. S. Tucker, J. L. Weiland, E. Wollack, and E. L. Wright, “Seven-Year Wilkinson Microwave Anisotropy Probe (WMAP) Observations: Sky Maps, Systematic Errors, and Basic Results,” *The Astrophysical Journal Supplement Series*, vol. 192, no. 2, p. 14, Jan. 2011.

- [15] A. M. Tillmann and M. E. Pfetsch, “The computational complexity of the restricted isometry property, the nullspace property, and related concepts in compressed sensing,” *Information Theory, IEEE Transactions on*, vol. 60, no. 2, pp. 1248–1259, 2014.
- [16] A. S. Bandeira, E. Dobriban, D. G. Mixon, and W. F. Sawin, “Certifying the restricted isometry property is hard,” *IEEE transactions on information theory*, vol. 59, no. 6, pp. 3448–3450, 2013.
- [17] T. Strohmer and R. W. Heath, “Grassmannian frames with applications to coding and communication,” *Applied and computational harmonic analysis*, vol. 14, no. 3, pp. 257–275, 2003.
- [18] P. Delsarte, J.-M. Goethals, and J. J. Seidel, “Spherical codes and designs,” *Geometriae Dedicata*, vol. 6, no. 3, pp. 363–388, 1977.
- [19] H. Zörlein and M. Bossert, “Coherence optimization and best complex antipodal spherical codes,” *IEEE Transactions on Signal Processing*, vol. 63, no. 24, pp. 6606–6615, 2015.
- [20] D. J. Love, R. W. Heath, and T. Strohmer, “Grassmannian beamforming for multiple-input multiple-output wireless systems,” *IEEE transactions on information theory*, vol. 49, no. 10, pp. 2735–2747, 2003.
- [21] M. Elad, “Optimized projections for compressed sensing,” *IEEE Transactions on Signal Processing*, vol. 55, no. 12, pp. 5695–5702, 2007.
- [22] E. J. Candès and M. B. Wakin, “An introduction to compressive sampling,” *Signal Processing Magazine, IEEE*, vol. 25, no. 2, pp. 21–30, 2008.
- [23] J. A. Tropp, “Greed is good: Algorithmic results for sparse approximation,” *IEEE Transactions on Information theory*, vol. 50, no. 10, pp. 2231–2242, 2004.
- [24] R. Balan, B. G. Bodmann, P. G. Casazza, and D. Edidin, “Painless reconstruction from magnitudes of frame coefficients,” *Journal of Fourier Analysis and Applications*, vol. 15, no. 4, pp. 488–501, 2009.
- [25] Y. C. Eldar and G. D. Forney, “Optimal tight frames and quantum measurement,” *IEEE Transactions on Information Theory*, vol. 48, no. 3, pp. 599–610, 2002.
- [26] A. J. Scott, “Tight informationally complete quantum measurements,” *Journal of Physics A: Mathematical and General*, vol. 39, no. 43, p. 13507, 2006.
- [27] P. Drineas, M. Magdon-Ismail, M. W. Mahoney, and D. P. Woodruff, “Fast approximation of matrix coherence and statistical leverage,” *Journal of Machine Learning Research*, vol. 13, no. Dec, pp. 3475–3506, 2012.
- [28] M. Mohri and A. Talwalkar, “Can matrix coherence be efficiently and accurately estimated?” in *Proceedings of the Fourteenth International Conference on Artificial Intelligence and Statistics*, 2011, pp. 534–542.
- [29] L. Welch, “Lower bounds on the maximum cross correlation of signals (corresp.),” *IEEE Transactions on Information theory*, vol. 20, no. 3, pp. 397–399, 1974.
- [30] J. D. McEwen and Y. Wiaux, “A Novel Sampling Theorem on the Sphere,” *IEEE Transactions on Signal Processing*, vol. 59, no. 12, pp. 5876–5887, Dec. 2011.
- [31] I. B. Hagi, F. M. Fazi, and B. Rafaely, “Generalized Sampling Expansion for Functions on the Sphere,” *IEEE Transactions on Signal Processing*, vol. 60, no. 11, pp. 5870–5879, Nov. 2012.
- [32] J. D. McEwen, G. Puy, J.-P. Thiran, P. Vandergheynst, D. Van De Ville, and Y. Wiaux, “Sparse image reconstruction on the sphere: implications of a new sampling theorem,” *Image Processing, IEEE Transactions on*, vol. 22, no. 6, pp. 2275–2285, 2013.
- [33] Y. F. Alem, D. H. Chae, and R. A. Kennedy, “Sparse signal recovery on the sphere: Optimizing the sensing matrix through sampling,” in *2012 6th International Conference on Signal Processing and Communication Systems*, Dec. 2012, pp. 1–6.

- [34] Y. F. Alem, S. M. A. Salehin, D. H. Chae, and R. A. Kennedy, "Sparse recovery of spherical harmonic expansions from uniform distribution on sphere," in *2013, 7th International Conference on Signal Processing and Communication Systems (ICSPCS)*, Dec. 2013, pp. 1–5.
- [35] Y. F. Alem, D. H. Chae, and S. M. A. Salehin, "Sparse recovery on sphere via probabilistic compressed sensing," in *2014 IEEE Workshop on Statistical Signal Processing (SSP)*, Jun. 2014, pp. 380–383.
- [36] R. A. Kennedy and P. Sadeghi, *Hilbert space methods in signal processing*, 2013.
- [37] E. Wigner, *Group theory: and its application to the quantum mechanics of atomic spectra*. Elsevier, 2012, vol. 5.
- [38] J. Bourgain, S. Dilworth, K. Ford, S. Konyagin, and D. Kutzarova, "Explicit constructions of RIP matrices and related problems," *Duke Mathematical Journal*, vol. 159, no. 1, pp. 145–185, Jul. 2011.
- [39] S. Dirksen, G. Lécué, and H. Rauhut, "On the gap between restricted isometry properties and sparse recovery conditions," *IEEE Transactions on Information Theory*, 2016.
- [40] G. Lohöfer, "Inequalities for the associated Legendre functions," *Journal of Approximation Theory*, vol. 95, no. 2, pp. 178–193, 1998.
- [41] D. J. Griffiths, *Introduction to quantum mechanics*. Cambridge University Press, 2016.
- [42] M. E. Rose, *Elementary theory of angular momentum*. Courier Corporation, 1995.
- [43] A. R. Edmonds, *Angular momentum in quantum mechanics*. Princeton University Press, 2016.
- [44] L. C. Biedenharn and J. D. Louck, *Angular momentum in quantum physics: theory and application*. Cambridge University Press, 1984.
- [45] A. Bangun, A. Behboodi, and R. Mathar, "On the maximum discrete inner product of wigner d-functions with application in compressed sensing," *To appear*.
- [46] —, "Coherence bounds for sensing matrices in spherical harmonics expansion," in *IEEE International Conference on Acoustics, Speech and Signal Processing (ICASSP'18)*. Calgary, Canada: IEEE, Apr 2018.
- [47] V. Torczon, "On the convergence of pattern search algorithms," *SIAM Journal on optimization*, vol. 7, no. 1, pp. 1–25, 1997.
- [48] E. B. Saff and A. B. Kuijlaars, "Distributing many points on a sphere," *The mathematical intelligencer*, vol. 19, no. 1, pp. 5–11, 1997.
- [49] J. Cui and W. Freeden, "Equidistribution on the sphere," *SIAM Journal on Scientific Computing*, vol. 18, no. 2, pp. 595–609, 1997.
- [50] R. Swinbank and R. James Purser, "Fibonacci grids: A novel approach to global modelling," *Quarterly Journal of the Royal Meteorological Society*, vol. 132, no. 619, pp. 1769–1793, 2006.
- [51] Y. Zhang, J. Yang, and W. Yin, "YALL1: Your algorithms for L1," *MATLAB software*, <http://www.caam.rice.edu/~optimization/L1>, vol. 1, 2010.
- [52] J. E. Hansen, *Spherical near-field antenna measurements*. IET, 1988, vol. 26.
- [53] R. Cornelius, A. A. Bangun, and D. Heberling, "Investigation of different matrix solver for spherical near-field to far-field transformation," in *Antennas and Propagation (EuCAP), 2015 9th European Conference on*. IEEE, 2015, pp. 1–4.
- [54] C. Culotta-López, D. Heberling, A. Bangun, A. Behboodi, and R. Mathar, "A compressed sampling for spherical near-field measurements," in *2018 AMTA 2018 Proceedings*. IEEE, 2018, pp. 1–6.
- [55] U. Haagerup and H. Schlichtkrull, "Inequalities for jacobi polynomials," *The Ramanujan Journal*, vol. 33, no. 2, pp. 227–246, 2014.